Fuel 406 (2026) 136933

Contents lists available at ScienceDirect

Fuel

journal homepage: www.elsevier.com/locate/fuel

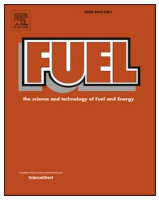

Full Length Article

# Chemical hot gas cleaning of Alkali, Chlorine, and Sulphur species in a sorption enhanced gasification process at 650 °C

Markus Kopsch [a,*], Patrick Schuster [a], Elena Yazhenskikh [a], Jürgen Sitzmann [b], Michael Müller [a]

[a] Institute of Energy Materials and Devices (IMD-1), Wilhelm-Johnen Straße, 52428 Jülich, Forschungszentrum Jülich GmbH, Germany
[b] Calida Cleantech GmbH, Adlerstraße 2, 91560 Heilsbronn, Germany

ARTICLE INFO

*Keywords:*
Hot Gas Conditiong (HGC)
Sorption
Sorption Enhanced Gasification (SEG)

ABSTRACT

The European GICO-Project aimed to develop an advanced approach to convert energy from biomass into biofuel and on-demand power production. In the GICO-Process, a $H_2$-rich hot gas stream of a gasifier operating at 650 °C has to be cleaned from inorganic contaminants, e.g. $H_2S$, HCl, and KCl, to protect downstream equipment, e.g. membranes, SOFC and a plasma reactor from corrosion. The use of CaO as a primary sorption material in the gasification reactor reduces the $CO_2$ amount by forming $CaCO_3$. Moreover, CaO reduces the $H_2S$ and HCl concentration in the gasifier by forming CaS, respectively $CaCl_2$. However, previous studies have shown that these reactions are not sufficient to reduce the $H_2S$ and HCl concentrations below the demanded 1 $ppm_v$ goal. Thus, secondary hot gas cleaning is necessary. As standard sorbents are only used at temperatures up to 600 °C, further consideration of new sorbents developed and investigated in this work is of particular interest.

Thermodynamic model calculations and sorption experiments in lab-scale furnaces were conducted to determine if chemical hot gas cleaning concepts can effectively remove sour gas and alkali components from the syngas leaving a gasification unit operating at 650 °C. In contrast to other studies, gases such as $CO_2$, $H_2O$, $H_2$, and CO were not substituted in the sorption experiments. This realistic gas composition represents a novel approach at 650 °C, allowing for more representative and reliable experimental results. Using a mass spectrometer, it was possible to record the $H_2$, $CO_2$, $H_2S$, and HCl concentrations during the sorption experiments simultaneously, although the input concentrations of the gas components ($H_2$: 72 vol-%, $CO_2$: 1 vol-%, $H_2S$: 60 $ppm_v$ and HCl: 40 $ppm_v$) were differing strongly. Zinc titanate, as a conventional sulfur sorbent, reduced the $H_2S$ concentration in the experiments to around 7 $ppm_v$. Ba-, Sr-, and Ce-containing sorbents achieved $H_2S$ concentrations below 1 $ppm_v$ for several hours, which should be sufficient to prevent poisoning of the nickel catalyst. 6 aluminosilicates, i.e. Bauxite, Clinoptilolite, Kaolin, Bentonite, Montmorillonite, and Cat litter, have been proven to be suitable for KCl reduction to values below 1 $ppm_v$.

## 1. Introduction

Although gasification of biomass is technically advanced and has been implemented on a large scale several times, one of the main existing challenges is the development of a resource-saving and cost-effective hot gas conditioning (HGC) system to produce highly pure synthesis gas [1–3]. Impurities contained in syngas include particulates, tars, and inorganics, posing environmental risks. HGC can be used to reduce organic (e.g. tars) and inorganic contaminants (e.g. sulfur, chlorine, alkali metals) released from low-cost fuels during gasification. $H_2S$, KCl, and HCl are the main contaminants produced during biomass gasification [4,5]. Moreover, there is a huge difference in terms of contaminant concentration ranging from a few $ppm_v$ to over 1000 $ppm_v$ depending on the biomass.

The EU project GICO ("Gasification Integrated with $CO_2$ capture and conversion") [6] focused on the development of small to medium scale residual biomass plants based on sorption enhanced gasification. The use of CaO sorbents in a low-temperature-fluidised-bed-gasifier operating at 650 °C shifts the thermodynamic equilibrium towards higher $H_2$ concentrations (from approximately 40 % $H_2$ to 75 % $H_2$) which is beneficial for the operation of a high temperature fuel cell. Simultaneously, a $CO_2$-rich gas stream is produced by calcination of the

* Corresponding author.
*E-mail address:* m.kopsch@fz-juelich.de (M. Kopsch).

https://doi.org/10.1016/j.fuel.2025.136933
Received 31 March 2025; Received in revised form 28 August 2025; Accepted 20 September 2025
Available online 25 September 2025

resulting calcium carbonate at 920 °C allowing for carbon capture and utilization. In this process, two hot gas streams need to be purified to protect downstream equipment like membranes, fuel cells, and plasma reactors.

In the GICO-process, different sulfur compounds are present in gases in different operating units, with $SO_2$ predominating in calciner gases and $H_2S$ being a by-product of gasification. However, small quantities of each product can be found in either unit. Consequently, it is important to distinguish between HGC methods that remove $SO_2$ from calciner gases and those that remove $H_2S$ from the gasifier gases. Since $H_2S$ is one of the most problematic sulfur contaminants under gasification conditions, its removal is necessary. However, currently used techniques like wet scrubbing are producing by-products that need to be further treated. Moreover, they are energy intense due to the thermal management (cooling and heating steps) of the feed stream.

Therefore, investigations on chemical HGC were conducted and showed that metal oxides are suitable for sulfur reduction [7–9]. Several Mn-, Ca-, Cu-, Fe-, and Zn-based sorbents with high sulfur capacity have been developed in the temperature range up to 600 °C [10]. It is possible to achieve $H_2S$ concentrations of 1–5 $ppm_v$ for Cu-based sorbents to 10 $ppm_v$ for zinc ferrites in gasifier-derived gases [9,11]. Although reaction (1) shows that the sorption reaction is sensitive to water, many syngases used for $H_2S$ sorption investigations were only balanced with $N_2$ or He [12–18].

$$MO_{(s)} + H_2S_{(g)} \leftrightarrow MS_{(s)} + H_2O_{(g)} \quad (1)$$

In order to fulfill the requirement of a nickel catalyst for 1 $ppm_v$ $H_2S$ in the high temperature range of 800–900 °C, investigations were carried out with barium-based sorbents. Thermodynamic calculations indicated that stabilized Ba sorbents should retain 1 $ppm_v$ $H_2S$, therefore the stabilization of the sorbent by CaO was investigated [19].

CaO-BaO shows low solubility at temperatures above 1200 °C. Therefore, in previous studies a sorbent was prepared from a mixture of BaO and CaO. The sorbent reduced the $H_2S$ concentrations to values below 0.5 $ppm_v$ in the temperature range of 800–900 °C. The XRD analysis confirmed the stabilization effect by the appearance of a BaS phase in the sorbent, which should normally be unstable under these conditions. At temperatures below 760 °C, the remaining $H_2S$ concentration increased strongly due to the carbonization of the sorbent [10].

Another potential second-generation sorbent for high-temperature gas desulfurization that has been studied is cerium oxide. Reversible adsorption of $H_2S$ on cerium oxide surfaces has been demonstrated over many cycles at temperatures as high as 800 °C [20,21]. Despite the fact that $CeO_2$ will react with $H_2S$, the reaction thermodynamics do not allow $H_2S$ target levels of about 20 $ppm_v$ to be achieved. $CeO_2$ is reduced at high temperatures to a nonstoichiometric oxide, $CeO_n$ ($n < 2$), which is superior to $CeO_2$ in removing $H_2S$. As a function of temperature, pressure, feed gas composition, and flow rate, the reduction and sulfidation reactions were studied in fixed-bed reactors.

$Ce_2O_3$ forms an oxysulfide with $H_2S$, but also $Ce_2S_3$ (see reactions 2–5). The $H_2S$ vapor pressure over $Ce_2S_3$ is greater than the vapor pressure of $H_2S$ over $Ce_2O_2S$.

$$2CeO_{2(s)} + H_{2(g)} \rightarrow Ce_2O_{3(s)} + H_2O_{(g)} \quad (2)$$

$$2CeO_{2(s)} + H_2S_{(g)} + H_{2(g)} \rightarrow Ce_2O_2S_{(s)} + 2\,H_2O_{(g)} \quad (3)$$

$$Ce_2O_{3(s)} + H_2S_{(g)} \rightarrow Ce_2O_2S_{(s)} + H_2O_{(g)} \quad (4)$$

$$Ce_2O_{3(s)} + 3H_2S_{(g)} \rightarrow Ce_2S_{3(s)} + 3\,H_2O_{(g)} \quad (5)$$

It has been shown that it is marginally more effective to produce $CeO_n$ as a separate step before reduction rather than simultaneously combined reduction and sulfidation. Despite this, both approaches were able to reduce $H_2S$ below the levels of 20 $ppm_v$ [20]. Table 1 summarizes the estimated tolerance limits for $H_2S$ that are expected to severely affect solid oxide fuel cells (SOFC) performance.

**Table 1**
Tolerance limits of inorganic contaminants for SOFC [22,23].

| Contaminant | Concentration [$ppm_v$] |
|---|---|
| $H_2S$ | 1–3 |
| HCl | 10–200 |
| Alkali | 10–200 |

However, lower concentrations of detrimental inorganic species in the syngas can not only be achieved by gas purification but also by impurity retention. Additives, such as lime, dolomite, or kaolin to reduce the release of sulfur and alkali species can be added to the fuel [24,25]. In conventional direct combustion processes, the most common technology to reduce sulfur at high temperature revolves around pulverizing $CaCO_3$ or dolomite, which is then fed into the combustion chamber. This means that $SO_2$ is removed right after combustion, before any gaseous material is produced. In general, it can be concluded that at higher temperatures (approximately 800 °C) $CaSO_4$ will be produced (reaction (6), while at lower temperatures, in the 450–800 °C region, the solid products are CaS and $CaSO_3$ (reaction (7) as well as $CaSO_4$ [9].

$$\boldsymbol{CaO_{(s)} + SO_{2(g)} + 0.5O_{2(g)} \rightarrow CaSO_{4(s)}} \quad (6)$$

$$\boldsymbol{CaCO_{3(s)} + SO_{2(g)} \rightarrow CaSO_{3(s)} + CO_{2(g)}} \quad (7)$$

$CaSO_4$ has a molar volume three times greater than CaO. Therefore, the molar volume of $CaSO_4$ produced during sulfidation will exceed the molar volume of CaO consumed, resulting in an increase in the amount of pore blockage that gradually eliminates $SO_2$ access to the active surface of CaO [9].

Alkali sorption experiments on aluminosilicates (bauxite, bentonite, kaolinite, etc.) have been undertaken in various temperature ranges over the past few decades [26,27]. Concentrations of a few hundred $ppb_v$ were achieved for several hours at 800 °C [10]. However, reaction (8) indicates the necessity of water [28,29]. Without water, the sorption reaction cannot take place.

$$Al_2O_3{\cdot}xSiO_{2(s)} + 2AlkCl_{(g)} + H_2O_{(g)} \leftrightarrow 2AlkAlO_2{\cdot}xSiO_{2(s)} + 2HCl_{(g)} \quad (8)$$

Moreover, several studies have been conducted to model the capture of K-species on Al-Si additives in literature [30]. However, the current models have some limitations. One common issue is that many models do not have a maximum limit to the capture value, which makes them unsuitable for use in a pulverised fuel power plant. Additionally, some models do not consider gas phase reactions (e.g. between KCl and $H_2O$ to form KOH), which can introduce errors when considering reactive species like KCl. Another drawback is the lack of consideration for multi-component sorption, where both KOH and KCl may be present in the gas phase and could potentially compete with each other in sorption reactions.

Although it is a modest air pollutant, HCl gas is troublesome because of its high solubility and corrosive nature [31,32]. That is the reason why its removal is an important issue. Studies on Ca-based sorbents indicated a high conversion rate for HCl between 400–650 °C [33–35]. Reactions (9) and (10) show the mechanisms for HCl sorption on CaO.

$$CaO_{(s)} + 2HCl_{(g)} \leftrightarrow CaCl_{2(s)} + H_2O_{(g)} \quad (9)$$

$$CaCO_{3(s)} + 2HCl_{(g)} \leftrightarrow CaCl_{2(s)} + H_2O_{(g)} + CO_{2(g)} \quad (10)$$

Thermodynamic investigations have shown that only a concentration of 600 $ppm_v$ can be achieved during HCl sorption on Ca-based sorbents above 800 °C [36]. However, in a dry atmosphere, HCl has been reduced below 1 $ppm_v$ [37,38] by stabilizing calcium in an aluminosilicate phase (hydrogrossular). Further studies are required to determine the HCl concentration achieved by the hydrogrossular in a humid reducing atmosphere [4]. Sufficient HCl removal with $Na_2CO_3$, $K_2CO_3$, and dried

distillers grains with solubles (DDGS) ash has also been demonstrated for temperatures up to 550 °C at Forschungszentrum Jülich [39]. To determine kinetically effects, a gas stream consisting of 66 % He, 4 % $H_2$, and 30 % $H_2O$ was varied between 2–4 l/min. The length of the sorbent fill varied from 25 mm to 100 mm. The HCl sorption on $Na_2CO_3$ and $K_2CO_3$ at temperatures between 400 °C and 550 °C showed that this reaction is kinetically limited. In order to prevent the limitation through kinetics, the space velocity has to be reduced to 4900 $h^{-1}$ for the $Na_2CO_3$ sorbent and to 3750 $h^{-1}$ for the $K_2CO_3$ sorbent. However, HCl concentrations of 1 $ppm_v$ are achievable below these space velocities.

The aim of this work was to investigate suitable sorbents for hot gas cleaning downstream of the gasifier. The hot gas cleaning system should operate at 650 °C, just like the gasifier itself, in order to avoid heat losses. The fact that the stream leaving the gasifier has a low $CO_2$ concentration due to the reaction with CaO and a high $H_2$ concentration due to the water gas shift reaction was given special consideration when selecting suitable sorbents. Because the sorptive removal of KCl has already been tested with aluminosilicates at higher temperatures, this work focused more on the removal of $H_2S$.

## 2. Modeling and experimental section

A model for describing both the release and the removal of trace substances in syngases was created. The aim was to determine the limits of sorptive alkali and sour gas removal. For the thermodynamic equilibrium calculations, FactSage [40] with the in-house developed oxide database GTKT [41] and the commercial database SGPS were used. While the model for the release calculations for several biomass fuels can be found in [42], Fig. 1 shows the calculation scheme for the subsequent hot gas cleaning. The resulting gas compositions from the release model was used as input for the present calculations. The concept consists of an alkali and a sour gas cleaning unit. The gas is brought into contact with various sorption materials. The sorbents were added in stoichiometric excess, so that the resulting concentrations are the minimum achievable with the respective sorbents and temperature. Moreover, no further gas–solid reactions can occur. Since HCl is released during alkali cleaning with aluminosilicates (reaction (8), the sour gas cleaning unit must be located afterwards.

### 2.1. Experimental setup and sorbent materials for KCl sorption

Except for the gas analysis, the experimental setups for the KCl sorption and the sour gas sorption were almost identical: A synthetically mixed syngas loaded with impurities was led through a sorbent bed in a tube furnace. This type of experimental setup has been used successfully in several previous studies [43–45]. All sorption experiments were conducted as fixed bed investigations at atmospheric pressure. The KCl sorption tests were stopped after 20 h since no increase in the corresponding signal could be detected.

The KCl sorption experimental setup consisted of a tube furnace with five independent heating zones. A high-density $Al_2O_3$-tube was used as the reaction tube. This material does not bind any alkalis at temperatures below 1000 °C. The KCl concentration was determined by molecular beam mass spectrometry (MBMS) as described in detail in [18].

Since previous thermodynamic calculations showed that the substitution of a simulated flue gas by helium has no influence on the KCl sorption [4,46], the syngas was synthetically mixed from 10 % $H_2$ and 83 % He. The gas stream was further loaded with 7 % $H_2O$ by flowing through a vaporizer. The gas mix (4 l/min) flowed through a flange into the cold end of the $Al_2O_3$ tube.

The $Al_2O_3$ tube had an inner diameter of 25 mm and a length of 870 mm. It was installed horizontally in a 5-zone furnace with an additional heating at the outlet. The additional heating was used to prevent the KCl from condensing at the inlet of the MBMS. The syngas was loaded with approximately 25 $ppm_v$ KCl shortly after flowing into the $Al_2O_3$ pipe by overflowing a 750 °C hot $Al_2O_3$ boat filled with KCl (alkaline source). The contact surface of the KCl with the syngas stream was approximately 900 $mm^2$.

The KCl loaded syngas then flowed through the bed of an aluminosilicate sorbent at 650 °C. To completely cover the pipe cross-section with sorbent material, the sorbent was pressed between two $Al_2O_3$-frits. The frits had a material thickness of 10 mm and consisted of a coarse-pored high-temperature $Al_2O_3$-foam. To reduce the flow resistance the sorbent was fractionated to a grain size between 1.6 and 4 mm. Approximately 30 g of sorbent were used per bed corresponding to a bed length of 50 mm.

The experimental setup such as syngas composition, syngas volume flow, general settings of the MBMS (ionization voltage, multiplier voltage, optics) was kept constant.

The chemical composition and the specific surface areas of the sorbents are given in Table 2 and Table 3. Before the BET measurement, the samples were outgassed by heating in a vacuum at 300 °C for 1 h. The materials used for alkali sorption were aluminosilicates differing in $Al_2O_3$ and $SiO_2$ content. Except for the bauxite, the $SiO_2/Al_2O_3$ ratio is bigger than 1. All sorbents listed in Table 2, except Boke Bauxite and Cat litter, were prepared from powder. The powder was mixed with water and formed into pellets. The pellets were then exposed in $Al_2O_3$ crucibles for 5 h at 650 °C in an air atmosphere. The sorbents were fractionated afterwards to a particle size of 1.6 to 4 mm. Cat litter and Boke Bauxite samples were still available from previous experiments and were only fractionated accordingly.

Calibration measurements were carried out to correlate the signal intensity measured at the MBMS with the respective KCl concentrations. The experimental setup corresponded to the one for KCl sorption, with

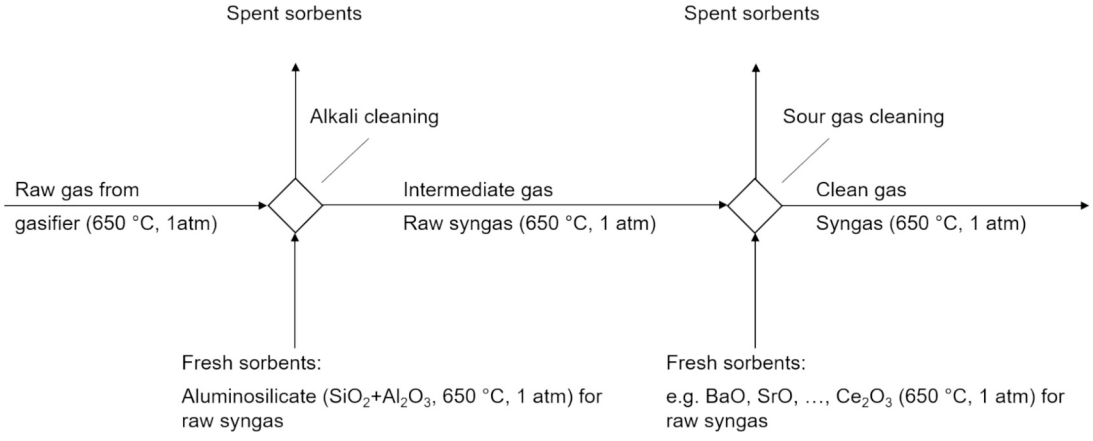


**Fig. 1.** Schematic representation of the HGC calculations.

**Table 2**
Chemical composition of the KCl sorbents [wt-%].

| Sorbent | $Al_2O_3$ | $SiO_2$ | $Fe_2O_3$ | $K_2O$ | $Na_2O$ | CaO | MgO | BaO | Total |
|---|---|---|---|---|---|---|---|---|---|
| Boke-Bauxite | 75 | 1.3 | 17.4 | – | – | – | – | – | 93.8 |
| Clinoptilolite | 12.8 | 76.2 | 0.3 | 3.5 | 1 | 2.3 | 0.6 | 0.1 | 96.8 |
| Kaolin | 47.2 | 58.6 | 0.8 | 2.2 | 0.1 | 0.1 | 0.3 | – | 109.4 |
| Bentonite | 17.9 | 64 | 1.1 | 0.5 | 3.1 | 0.4 | 2.8 | 0.1 | 89.9 |
| Cat litter | 0.2 | 51.1 | – | – | – | 20.3 | 2.2 | – | 73.9 |
| Montmorillonite | 19.5 | 61 | 0.9 | 1.4 | 0.3 | 0.6 | 3.7 | – | 87.4 |
| Foam | 94.1 | 5.5 | – | 0.5 | 0.5 | – | 0.1 | – | 100.7 |

**Table 3**
Specific surface areas [$m^2/g$] of the KCl sorbents.

| Sorbent | Specific Surface |
|---|---|
| Boke-Bauxite | 240.387 |
| Clinoptilolite | 26.366 |
| Kaolin | 15.761 |
| Bentonite | 15.538 |
| Cat litter | 95.083 |
| Montmorillonite | 60.417 |
| Foam | 1.358 |

the exception of the absence of sorbent. Furthermore, the temperature of the KCl source was increased step by step over several empty tube measurements. The KCl concentration in the syngas of an empty tube measurement was determined via the weight loss of the KCl source.

The masses 74 and 76 can be directly assigned to $K^{35}Cl^+$ and $K^{37}Cl^+$, respectively. Furthermore, the masses 35, 37, and 39 show the presence of the KCl fragments $^{35}Cl^+$, $^{37}Cl^+$, and $^{39}K^+$. Since chlorine reacts to HCl in the presence of water, signals could also be measured on masses 36 and 38. On the masses 56 and 58, which correspond to KOH and $K^{18}OH$ respectively, no significant signal increases could be observed. The quantification of the potassium chloride was carried out via mass 39, since it has the highest intensity.

### 2.2. Experimental setup and sorbent materials for $H_2S$ and HCl sorption

A test rig consisting of a glass reactor, various gas pipes and a water vaporizer was set up. A programmable furnace (AGNI Wärme- und Werkstofftechnik GmbH, Model: GHT-130–40-400-5H) was used to obtain a temperature-controlled operation for the sorption experiments. The furnace temperature was controlled via a PID controller acting on the temperature from the thermocouple integrated in the furnace (closed-loop control). Gas analysis was performed using mass spectrometry (MAX300, Extrel). The gas composition in the $H_2S$-sorption experiments was set to 73 % $H_2$, 13 % Ar, 7 % $H_2O$, 1 % $CO_2$, 6 % CO, 60 $ppm_v$. This composition was based on FactSage-equilibrium calculations of a synthesis gas leaving a biomass gasifier operated at 650 °C. Since the $H_2S$ sorption can be influenced by several syngas components, the $H_2S$ was mixed in with CO (0.1 %). The inert components ($N_2$) and the hydrocarbons (mainly $CH_4$) were substituted by Ar. Because of the expected low $H_2S$ concentration of the gas after $H_2S$ purification, the $H_2S$ signal was determined with an electron multiplier. For the remaining signals, a faraday detector was used.

The $H_2S$ sorption measurements always proceeded in the same way. First, the glass reactor filled with sorption material was flooded with argon. In the second step, the reactor was disconnected from the gas supply by closing the valves immediately upstream and downstream of the reactor. The argon gas flow was then used to purge the pipelines (the gas flow was not yet loaded with water). The CO/$H_2S$ supply was then started. Since the $H_2S$ molecule adsorbed well on surfaces, a steady-state signal was obtained by waiting until the $H_2S$ signal plateaued. Next, the $CO_2$ stream and the $H_2$ stream were switched on. The valve to the water supply was opened and the heating of the water started. The gas flow is thus directed onto the water surface from above. After the first steam bubbles appeared, the gas ($H_2$, $CO_2$, Ar) was directed through the water and loaded. Subsequently, the gas mixture was passed through the reactor. As soon as the sorption material was saturated and the $H_2S$ and HCl concentration increased, the sorption experiments were stopped. At the end of each experiment, the water supply was stopped and the reactor was flooded with argon.

Similar to the KCl sorption experiments, the HCl contamination was generated by evaporating a solid, i.e., $NH_4Cl$, in an $Al_2O_3$ boat at a fixed temperature during the experiment. The filled boat was attached to the glass rod of the reactor with a metal wire. To fix the sorption material in the glass tube, a foam was used as in the KCl sorption experiments (see Fig. 2).

The experimental setup for HCl sorption differed only slightly from the experimental setup for $H_2S$ sorption: Helium was used here for the substitution of $CH_4$ and $N_2$. This change was made because Ar has isotopes at masses 36 and 38 in addition to the main mass at 40. The main signal of HCl is at mass 36.

Since the temperature profile inside the furnace was very steep, the $NH_4Cl$ was evaporated upstream the furnace via a heating belt.

Table 4 lists all the chemicals used for HCl and $H_2S$ sorption. The degree of purity was over 98 % for all chemicals. The sorption properties of a commercially available lime (Sorbacal) from Rheinkalk were also investigated. The chemical composition is given in Table 5. The values for the oxides were calculated from the elements measured with ICP-OES. In previous studies, the CaO content was 98.1 wt-%. The lower percentage can be explained by the fact that $Ca(OH)_2$ and $CaCO_3$ have formed during storage.

In order to ensure a concentration of 1 $ppm_v$ $H_2S$ in the syngas, conventional sorption materials like ZnO could not be used, as these only show good sorption efficiency at temperatures below 600 °C. Therefore, the Sr- and Ba-based sorption materials developed by Stemmler at Forschungszentrum Jülich were included in the experiments. Stemmler's calculation showed that stabilized Ba-based sorbents keep the 1 $ppm_v$ concentration even in a temperature range between 800 °C and 900 °C [39].

There is a slight solubility of BaO and CaO at temperatures above 1200 °C [4,39,47]. Moreover, all CaO-SrO mixtures above 900 °C are forming a CaO-SrO solution phase. Since increased marginal solubilities exist, mixtures of 90 mol-% CaO and 10 mol–% SrO (or BaO), respectively 10 mol-% CaO and 90 mol-% SrO were used for $H_2S$ sorption.

For the preparation of the $H_2S$ and HCl sorbents, raw powder ($SrCO_3$, $ZnTi_2O_4$, $CeO_2$, …) was mixed with water and formed to pellets. For the preparation of the Sr- and Ba-based sorption material, carbonates were used. Preliminary thermo-gravimetric measurements showed that the decomposition reaction of $CaCO_3$ to CaO is completed at about 800 °C to 850 °C, while $SrCO_3$ is completely decomposed at about 1150 °C and $BaCO_3$ at 1200 °C. Therefore, the sorbents used in the sorption experiment were prepared at 1600 °C in platinum crucibles.

For the production of reduced ceria sorption material, raw powder of $CeO_2$ was mixed with water and heated in a 10 % $H_2$-Ar atmosphere at 1500 °C for 72 h. $Ce_2O_3$ is stable in air if it has been produced at temperatures above 1400 °C [48]. The specific surface area of the most highly reduced cerium oxide sample was determined to be 0.21 $m^2/g$.

The temperatures and exposure times of the other sorbents can be found in Table 6. To ensure a certain mechanical stability of the sorption

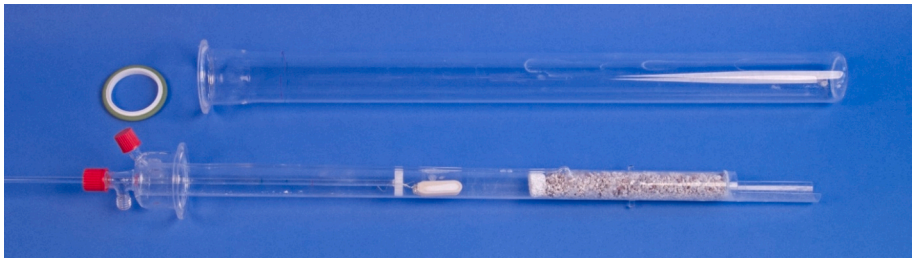

**Fig. 2.** Glass reactor filled with SrO with additional HCl source.

**Table 4**
List of chemicals used for $H_2S$ and HCl sorbents preparation.

| Chemical | Assay | Supplier | CAS Registry Number |
|---|---|---|---|
| $BaCO_3$ | ≥ 99 % | Thermo Scientific, Schwerte | 513–77-9 |
| $CaCO_3$ | ≥ 99.5 % | Thermo Scientific, Schwerte | 471–34-1 |
| $CeO_2$ | ≥ 99.5 % | Thermo Scientific, Schwerte | 1306–38-3 |
| $La_2O_3$ | ≥ 99.9 % | Thermo Scientific, Schwerte | 1312–81-8 |
| $SrCO_3$ | ≥ 98 % | Fischer Scientific, Geel (Belgium) | 1633–05-2 |
| $Y_2O_3$ | ≥ 99 % | Merck, Darmstadt | 1314–36-9 |
| $Zn_2TiO_4$ | ≥ 99.9 % | Thermo Scientific, Schwerte | 12036–43-0 |

**Table 5**
Chemical composition of Sorbacal [wt-%].

| Sorbent | $Al_2O_3$ | $SiO_2$ | $Fe_2O_3$ | CaO | MgO |
|---|---|---|---|---|---|
| Sorbacal | 0.2 | 1 | 0.2 | 62.1 | 0.6 |

**Table 6**
Manufacturing temperatures and duration.

| Sorbent | Temperature [°C] | Duration [h] |
|---|---|---|
| $La_2O_3$ | 1400 | 5 |
| $Zn_2TiO_4$ | 650 | 5 |
| $CeO_2$ | 1050 | 10 |
| $Y_2O_3$ | 1050 | 10 |

material, different temperatures and dwell times in the furnace were used depending on the sorption material. The specific surface areas of the sorbents are listed in Table 7.

As described earlier, the $H_2S$ signal was recorded by mass spectrometry. Before starting the $H_2S$ investigations, the signal intensities were correlated with the corresponding $H_2S$ concentrations. In analogy to the KCl calibration, empty pipe measurements were carried out.

Since a syngas purity of less than 1 $ppm_v$ $H_2S$ was aimed for, $H_2S$ concentrations of 60 $ppm_v$, 30 $ppm_v$, 10 $ppm_v$, 5 $ppm_v$, 2.5 $ppm_v$, 1 $ppm_v$, and 0 $ppm_v$ were chosen as calibration points. Since $H_2S$ was mixed with CO, a decrease in the $H_2S$ input was accompanied by a decrease in the CO input. The syngas fraction missing due to the reduction of the $H_2S$ concentration was substituted by Ar. A total flow rate of 2 l/min was used for the calibration. The empty tube measurements resulted in a linear correlation between $H_2S$ concentration and signal intensity at mass 34.

**Table 7**
Specific surface areas of the $H_2S$ and HCl sorbents [$m^2/g$].

| Sorbent | Specific surface |
|---|---|
| Sorbacal | 4.778 |
| $La_2O_3$ | 0.642 |
| $Zn_2TiO_4$ | 0.586 |
| $Y_2O_3$ | 1.761 |
| 90Ca10Ba | 0.878 |
| 90Ca10Sr | 0.242 |
| 10Ca90Sr | 0.466 |
| 100Sr | 0.209 |

According to the KCl and $H_2S$ calibration, a correlation between signal intensities and HCl concentrations was conducted prior to the HCl sorption experiments. An empty pipe calibration was carried out similar to the KCl calibration.

## 3. Results and Discussion

### 3.1. Modeling results.

Depending on biomass, the syngas leaving the gasifier contains approximately 20 $ppm_v$ $H_2S$, 160 $ppm_v$ HCl, and up to 22 $ppm_v$ alkali chlorides [42]. After sorptive alkali hot gas cleaning on aluminosilicates at 650 °C, the NaCl concentrations ranged up to 0.97 $ppb_v$, while the maximum KCl concentration was 1.5 $ppb_v$. With concentrations of up to 188 $ppm_v$, in the purified syngas, the concentration of HCl was the only chlorine species that increased significantly according to reaction (8). Since $H_2S$ does not react with aluminosilicates, its concentrations remained unchanged at 20 $ppm_v$.

Based on the results of the alkali cleaning calculations, further calculations for the sour gas cleaning were carried out. Therefore, several metals/metal oxides as well as natural occurring alkali and alkaline earth compounds had been considered.

The results (Fig. 3) show that SrO, BaO, and $Ce_2O_3$ were suitable to reduce the concentrations of $H_2S$ from approximately 20 $ppm_v$ to values below 1 $ppm_v$ (SrO: 2.8 ppb, BaO, 0.013 ppb, $Ce_2O_3$: 1 ppt) at 650 °C. These concentrations were all within the range of purities demanded for the use of SOFC in Table 1. From a thermodynamic point of view, gas purification can therefore be carried out in the way described. With the help of Zn-based sorption materials (ZnO and $Zn_2TiO_4$), the $H_2S$ concentration could be reduced to a few $ppm_v$ (ZnO: 5.1 $ppm_v$, $Zn_2TiO_4$: 10.4 $ppm_v$) at 650 °C.

Similar statements can also be made about the HCl sorption at 650 °C with the sorption materials mentioned. BaO and SrO sorbents could reduce the concentrations of HCl from around 188 $ppm_v$ to 2.8 $ppb_v$ and 0.37 $ppm_v$. $Ce_2O_3$ reduced the HCl amount to 17.7 $ppm_v$, while ZnO and $Zn_2TiO_4$ were not able to reduce the input concentration as expected. Fig. 3 shows another positive effect of BaO, SrO, and $Ce_2O_3$ on the syngas. The $CO_2$ concentrations of approximately 1 % could be further reduced. This also has the advantage of shifting the equilibrium to higher $H_2$ concentrations.

The sorption capacity of BaO- and SrO-based sorption materials with respect to $CO_2$, $H_2S$, and HCl can be seen positively over a wide temperature range (400–1000 °C). $Ce_2O_3$, on the other hand, lowered the HCl concentration significantly only up to about 700 °C.

According to these calculations, the barium, strontium, and cerium-based sorption materials result in low $H_2S$ and HCl concentrations. They are also temperature-stable at 650 °C and will be therefore investigated experimentally in the following.

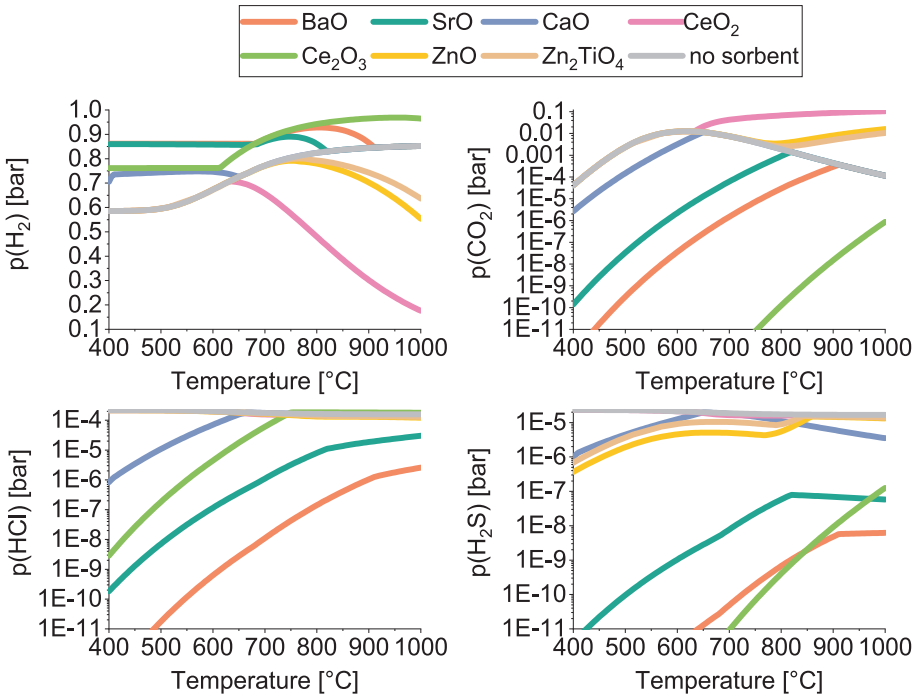


**Fig. 3.** Partial pressure of $H_2$, $CO_2$, HCl, and $H_2S$ after $H_2S$/HCl cleaning for different sorbents.

### 3.2. Experimental KCl sorption at 650 °C

As described, in all investigations for the KCl removal, a KCl-loaded syngas, was passed through a fixed bed. The achievable KCl concentration was determined in situ using a MBMS. Reaction (8) shows a dependence on the water content of the KCl concentration in the syngas. The gas mixture used in these experiments (83 % He, 10 % $H_2$, and 7 % $H_2O$) is thus a permissible simplification of the GICO syngas.

Fig. 4 shows the KCl concentration profiles of different sorbents. All tested sorbents reduced the KCl concentration to as low as 0.4 $ppm_v$ and thus, are suitable sorbents. The KCl concentrations when using Kaolin, Bentonite, Montmorillonite, and Clinoptilolite were below the detection limit.

### 3.3. Experimental $H_2S$ sorption at 650 °C

In all investigations on $H_2S$ cleaning, the syngases were passed through a fixed bed. The $H_2S$ signal of the purified gas was recorded by mass spectrometry (MS). Stemmler reported considerable delays in his measurements since the $H_2S$ molecule adsorbed well on surfaces [4]. Therefore, in this work the gas was fed into a separate circuit so that the surfaces of the gas pipes were saturated with $H_2S$ until shortly before the glass reactor. To shorten the saturation time, the $H_2S$ concentration in the gas was increased before opening the sorbent circuit. The experiment was started as soon as there was a steady-state signal.

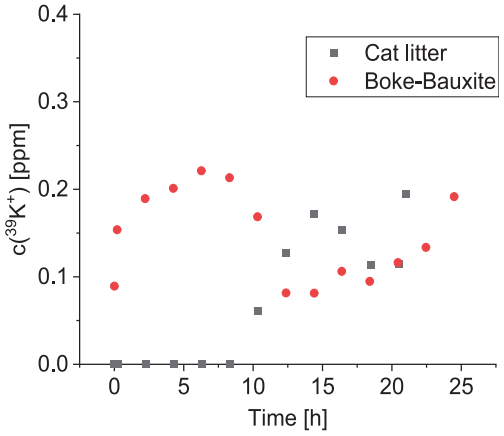


**Fig. 4.** KCl concentration after streaming through a sorbent bed at 650 °C (inlet concentration: 83 % He, 10 % $H_2$, 7 % $H_2O$, and 25 $ppm_v$ KCl, $V_{tot}$ = 4 l/min, 30 g sorbent).

In order to obtain a rough overview of the sorption behavior of the different sorbents, sorption experiments were carried out at a high flow rate (2 l/min). The most promising sorbents were then tested at a lower flow rate (200 ml/min) and with a longer sorption fill (100 g sorbent). Fig. 5 shows the $H_2S$ concentrations during the first 20 min of the $H_2S$ sorption experiments for different sorbents. The $CO_2$ intensity was also recorded. However, since the $CO_2$ concentration was not in the main focus of the investigations, the MS was not calibrated for $CO_2$ and the values are given as signal intensities, only.

Although $CO_2$ leaves the gasifier with a low concentration of around 1 % due to the sorption with CaO (calculated thermodynamic equilibrium), SrO and $Ce_2O_3$ decreased the concentration even a little further. However, a rise in the $CO_2$ signal could be observed after just a few minutes for these sorption materials. Parallelly, the $H_2S$ concentration increased. Therefore, $CO_2$ can be seen as a limiting factor in the conducted $H_2S$-sorption experiments: SrO reacts with $CO_2$ to form a carbonate ($SrCO_3$) while the reduced cerium oxide ($Ce_2O_3$) oxidizes ($CeO_2$). Both, the oxidation of the $Ce_2O_3$ and the carbonatization of SrO took place quickly, which is the reason that $H_2S$ could only be removed well for a short time.

For $Zn_2TiO_4$ no decrease of the $CO_2$ signal could be seen, as $ZnCO_3$ is only stable at temperatures up to approximately 300 °C. $Zn_2TiO_4$ lowered the $H_2S$ concentration to single-digit $ppm_v$ values for several hours despite a high flow rate. Because $La_2O_3$ has similar properties compared to $Ce_2O_3$ (molar mass, electronegativity), which according to the literature has a good $H_2S$ sorption effect [21,49,50], it was also used in the experiments. Since the 3-valent form of Lanthanum oxide ($La_2O_3$) and Yttria ($Y_2O_3$) are stable under gasification conditions, the $CO_2$ signals remained constant. However, $H_2S$ concentrations for $La_2O_3$ were as low as for $Zn_2TiO_4$. Moreover, $La_2O_2S$ was detected after the sorption experiment using XRD.

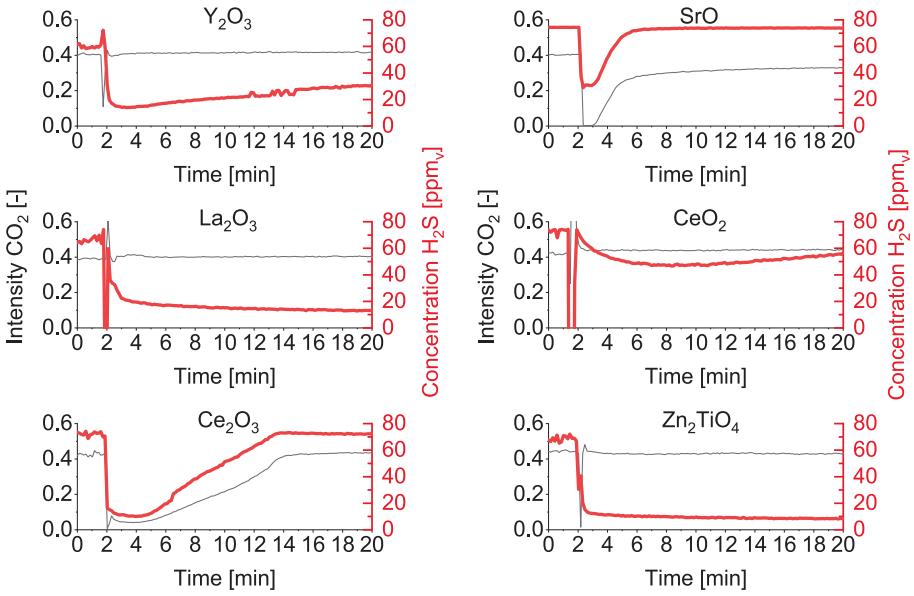


**Fig. 5.** Results of the mass spectrometric investigations: $CO_2$ intensity and $H_2S$ concentrations [$ppm_v$] of different sorbents. Inlet concentration: 73 % $H_2$, 13 % Ar, 7 % $H_2O$, 1 % $CO_2$, 6 % CO (60 $ppm_v$ $H_2S$), T = 650 °C, $V_{tot}$ = 2 l/min, 30 g sorbent.

As the $H_2S$ signal for SrO and $Ce_2O_3$ did not reach a plateau during sorption, it can be assumed that the gas has not yet reached its achievable purity. In order to give a better estimate of the sorption capacity, experiments were carried out with a reduced volume flow rate and a longer sorbent bed (100 g).

Furthermore, a stabilizing effect of CaO on SrO against carbonization was investigated by testing mixtures of 10 mol-% CaO, 90 mol-% SrO (10Ca90Sr), and 90 mol-% CaO, 10 mol-% SrO (90Ca10Sr). In addition, a 10 mol-% BaO, 90 mol-% CaO (90Ca10Ba) mixture was tested because it has achieved good results in Stemmler's work [10].

Fig. 6 (left) shows the $H_2S$ concentration when cerium oxide ($Ce_2O_3$) is used. $H_2S$ concentrations of less than 1 $ppm_v$ could be achieved for more than 5 h. After saturation, an extreme increase in the $H_2S$ concentration (approximately 170 $ppm_v$) could be seen for a short time, which slowly decreased. This is due to the fact that $H_2S$ was released again. The oxidized form ($CeO_2$) was more stable than the sulfides formed ($Ce_2O_2S$, $Ce_2S_3$).

The XRD analysis of the sorption material after the sorption experiment showed a single $CeO_2$ phase. No more sulfides or reduced cerium oxides could be detected.

The sorption with the BaO-sorbent (10Ba90Ca) also showed an increase in the $H_2S$ concentration above the initial concentration of 60 $ppm_v$ after deactivation of the sorption material (Fig. 6, right). The sorbent was also able to keep the $H_2S$ concentration below 1 $ppm_v$ for approximately 3 h.

Since both the Ba-sorbent and the Ce-sorbent also reacted with $CO_2$, the thermodynamic equilibrium shifted in the direction of extremely high hydrogen concentrations. However, no sulfide could be detected after the experiment due to the release of $H_2S$ after sorption. The XRD analysis of the sorption material showed that the formation of $CaCO_3$ was suppressed and that only $BaCO_3$ and CaO (Lime) were present (see Fig. 7).

As already described, 1 % $CO_2$ was selected for the input concentration in the experiments, because this is the minimum $CO_2$ concentration that can be achieved with CaO at 650 °C. Thus, it is confirmed that BaO in the sorbent was reducing the $CO_2$ concentration further.

To gain a better understanding of the deactivation behavior of 10Ba90Ca over time, the sorption experiment was stopped after 50, 100, 150, and 600 min. At these times, the syngas was replaced by argon. After the furnace had cooled down, the fixed bed was divided into ten

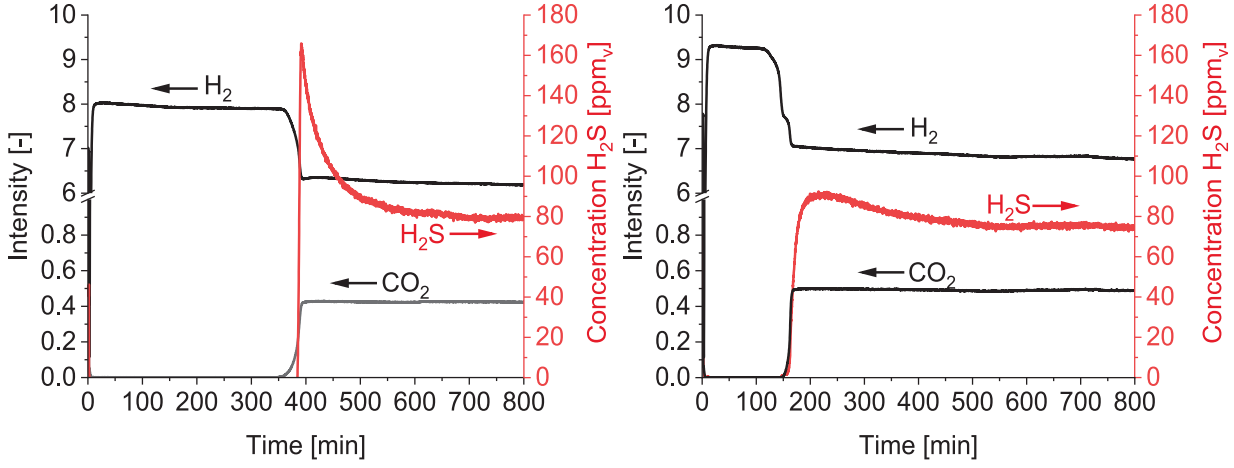


**Fig. 6.** Results of the mass spectrometric investigations: $CO_2$ intensity and $H_2S$ concentrations [$ppm_v$] of $Ce_2O_3$ (l.) and 10Ba90Ca (r.). Inlet concentration: 73 % $H_2$, 13 % Ar, 7 % $H_2O$, 1 % $CO_2$, 6 % CO (60 $ppm_v$ $H_2S$), T = 650 °C, $V_{tot}$ = 0,2 l/ min, 100 g sorbent.

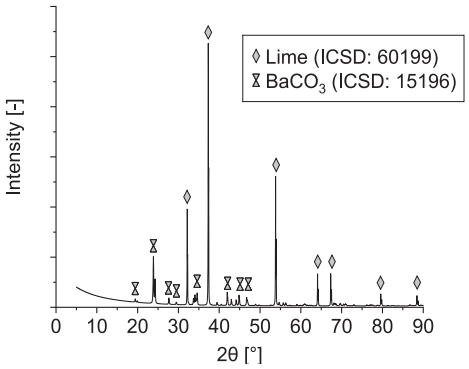


**Fig. 7.** XRD spectrum of 10Ba90Ca after sorption experiment.

fractions of equal size for chemical analysis.

Fig. 8 shows the evaluation of the elemental analysis. Sample position 1 refers to samples taken at the gas inlet side, while sample position 10 are samples taken at the gas outlet side.

It can clearly be seen that the C concentrations increased with increasing residence time in the reactor. Furthermore, higher C concentrations were observed at the reactor inlet. The C-analysis of an unloaded reference sample (dotted line) show that hardly any carbonates were present after sorbent production.

Since only gases such as $CO_2$ and CO were present as carbon sources, the increase in C concentration was due to the formation of $BaCO_3$ ($CaCO_3$ was not formed under these conditions). The higher C concentrations at the reactor inlet (sample position 1) compared to the reactor outlet (sample position 10) were due to the higher $CO_2$ concentrations at the reactor inlet. Lower amounts of $CO_2$ arrived at the back of the reactor with a time delay. After 50 min, approximately 50 % of the sorption material has reacted to $BaCO_3$.

For the sulfur concentration, there was also a corresponding drop in concentration along the bed. Only after 50 min an increase of the sulfur concentration for the samples that were located close to the gas outlet (sample positions 8–10) could be observed. Since the sulfur concentration at positions 8–10 has decreased over time while the C concentration has increased, it is reasonable to assume that the carbonates were more stable than the sulfur compounds and that the sulfur components (BaS) were driven further to the gas outlet. However, the leaching of the sulfur components did not occur completely.

Fig. 9 shows the $H_2S$ sorption process when using SrO. The 1 $ppm_v$ $H_2S$ target could not be achieved here. In contrast to $Ce_2O_3$ and the Ba-based sorption material, there was no extreme increase in the $H_2S$ concentration after deactivation by the $CO_2$.

Fig. 10 shows that $SrCO_3$ has been formed. Nevertheless, SrO could still be detected in the sample by XRD. Possibly only an external $SrCO_3$ layer has been formed. The inner part of the sorbent could still consist of SrO after the sorption experiment since the SrO sorbent had a small specific surface area (0.209 $m^2/g$, see Table 7.).

Fig. 11 shows the effect of CaO in a CaO-SrO mixture on the $H_2S$ concentration. It can be seen that in a CaO rich sorbent material (90Ca10Sr) the $CO_2$ concentration increased after a few minutes. As explained earlier, CaO cannot reduce $CO_2$ any longer. Since $CO_2$ and $H_2S$ intensities did not run parallel for both 90Ca10Sr and 10Ca90Sr, it is assumed that a mixed phase was present that reduced sulfur well. The XRD analysis of 90Ca10Sr showed that three $Ca_{1-x}Sr_xO_2$ mixed crystal

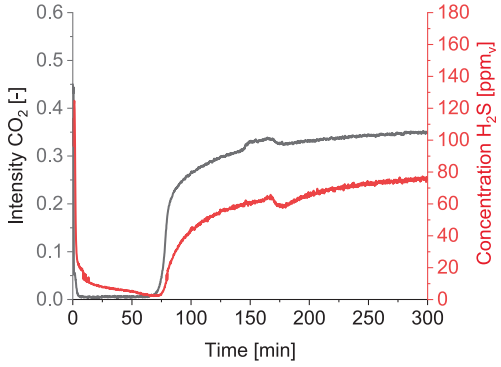


**Fig. 9.** Results of the mass spectrometric investigations: $CO_2$ intensity and $H_2S$ concentrations [$ppm_v$] of SrO. Inlet concentration: 73 % $H_2$, 13 % Ar, 7 % $H_2O$, 1 % $CO_2$, 6 % CO (60 $ppm_v$ $H_2S$), T = 650 °C, $V_{tot}$ = 0,2 l/min, 100 g sorbent.

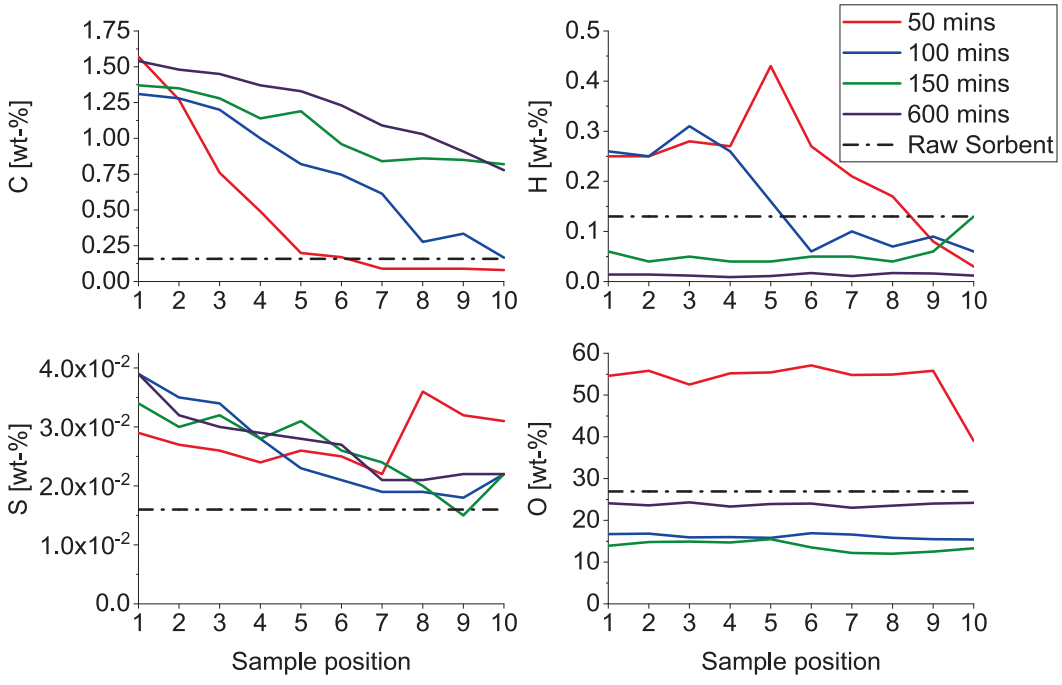


**Fig. 8.** Elemental analysis of 10Ba90Ca after 50, 100, 150, and 600 min of sorption time.

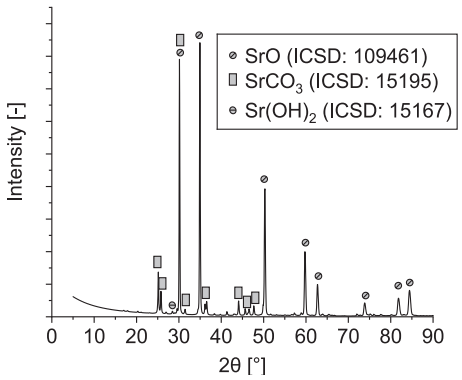


**Fig. 10.** XRD spectrum of SrO after sorption experiment.

phases were present, two rich in Ca with a = 4.838 Å and 4.859 Å and one rich in Sr with a = 5.112 Å (see Fig. 12).

### 3.4. Experimental HCl sorption at 650 °C

For the HCl sorption experiments, the two sorbents with the lowest equilibrium concentration according to model calculations (10Ba90Ca and SrO) were used. Similar to the KCl sorption experiments, the contamination was generated by evaporation of a source. In order to prevent the BaO sorption material from being deactivated by $CO_2$ during the heating phase of the $NH_4Cl$, the heating tape was turned on 7 h before the gas was passed through the glass reactor. Thus, HCl concentrated in the reactor and the equilibrium plateau was reached after only a few minutes. Compared to the $H_2S$ measurement (see Fig. 6, right), the HCl sorption showed an earlier increase of $CO_2$ after only 20 min (see Fig. 13, left).

As in the $H_2S$ sorption experiments, the sorption material in the HCl sorption experiments was deactivated by $CO_2$ in the syngas. The HCl signal in the 90Ca10Ba sorption measurement "shot up" beyond the input concentration and decreased again. This is similar to the $H_2S$ sorption measurement. It indicates that HCl was released.

The experimental procedure for SrO deviated a little. Here the heating tape, which was used for the evaporation of the $NH_4Cl$, was switched on two minutes before the glass reactor was opened. Since pure SrO was used here, the deactivation time was longer than for the Ba-based sorbent (see Fig. 13, right).

The tested sorbents were not able to noticeably reduce HCl concentrations. Both sorption materials could only reduce the HCl concentration for a short time by about 10–20 $ppm_v$: 10Ba90Ca lowered the HCl concentration for about 50 min from about 50 $ppm_v$ (input concentration) to about 30 $ppm_v$, SrO for about 100 min from about 50 $ppm_v$ (input concentration) to 40 $ppm_v$.

Moreover, neither for 10Ba90Ca, nor for SrO, Cl phases could be detected via XRD after the experiment. This is due to the low HCl concentration in the syngas and the short deactivation time. Therefore, the samples were analyzed with EDXRF. Chlorine could be detected in all samples. However, only a semi-quantitative observation was possible. In contrast to the spectral lines of the other elements, the intensity of the chlorine K-alpha line varied strongly, indicating inhomogeneous chlorine distribution in the sample.

### 3.5. Comparison of the FactSage model with experimental observations

Aluminosilicates showed good reduction potential for the alkali compounds KCl and NaCl in the calculations. This could be confirmed by the laboratory experiments with MBMS. The tested aluminosilicates reduced the KCl concentration to levels well below 1 $ppm_v$ in the experiments.

Similar observations could be made for the $H_2S$ sorption. According to the calculations, $Ce_2O_3$, BaO, and SrO ccould significantly reduce the $H_2S$ concentration below 1 $ppm_v$. This was also verified by the fixed bed sorption experiments. However, since the detection limit of the used mass spectrometer is about 1 $ppm_v$, no conclusions can be drawn about the exact actual purities of the gas for these three sorption materials. An increased $H_2$ concentration was also predicted for all three sorbents, which was also experimentally demonstrated. In comparison to the materials mentioned above, $Zn_2TiO_4$ was used as a conventional sorbent. Calculations and experiments proved that there is no deactivation by $CO_2$ here. The $H_2S$ concentration achieved in the sorption experiment was also within the range of the model (1–10 $ppm_v$).

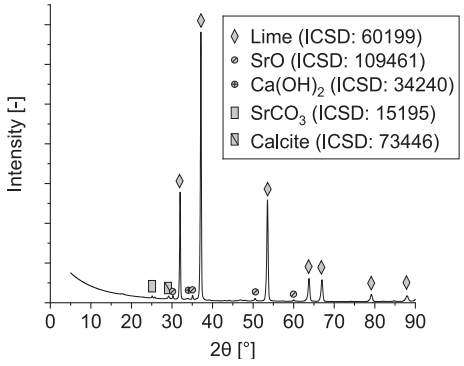


**Fig. 12.** XRD spectrum of 90Ca10Sr after sorption experiment.

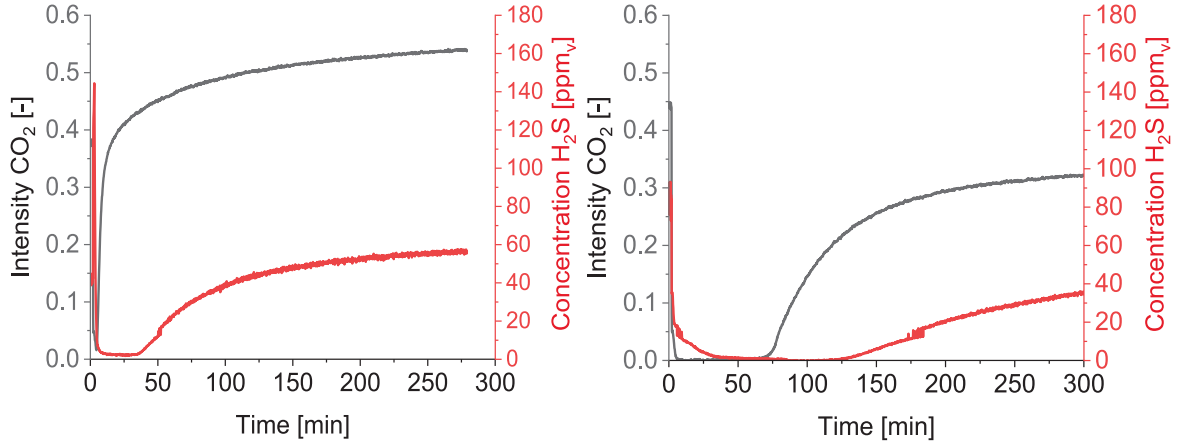


**Fig. 11.** Results of the mass spectrometric investigations: Influence of CaO on the stabilization of the Sr-sorbent. $CO_2$ intensity and $H_2S$ concentrations [$ppm_v$] of 90Ca10Sr (l.) and 10Ca90Sr (r.). Inlet concentration: 73 % $H_2$, 13 % Ar, 7 % $H_2O$, 1 % $CO_2$, 6 % CO (60 $ppm_v$ $H_2S$), T = 650 °C, $V_{tot}$ = 0,2 l/min, 100 g sorbent.

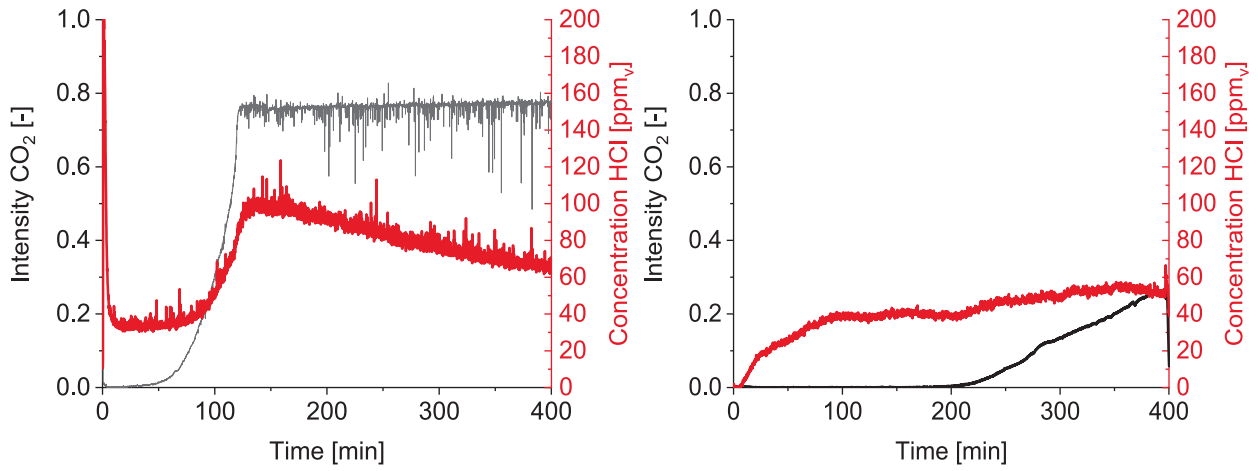


**Fig. 13.** Results of the mass spectrometric investigations: $CO_2$ intensity and HCl concentrations [$ppm_v$] of 10Ba90Ca (l.) and SrO (r.). Inlet concentration: 73 % $H_2$, 13 % Ar, 7 % $H_2O$, 1 % $CO_2$, 6 % CO, 50 $ppm_v$ HCl, T = 650 °C, $\dot{V}_{tot}$ = 0,2 l/min, 100 g sorbent.

Only the experiments for HCl sorption deviated strongly from the predictions. The tested sorbents could not really reduce HCl. This may be due to incorrect or insufficient data in the database and the non-consideration of kinematic effects, since only equilibria were covered by the model.

### 3.6. HGC concept for the GICO process

The present results indicate that the reduction of $H_2S$ at 650 °C using either $Ce_2O_3$, SrO or BaO is only possible if the syngas has a low $CO_2$ content, since these sorbents are deactivated by carbonation or oxidation. Therefore, a low $CO_2$ content is beneficial when utilizing $Ce_2O_3$, SrO or BaO for high-temperature sorption. However, the GICO experimental plant may not achieve this theoretical value in its fluidized bed. $CO_2$ concentrations between 3–5 % are expected. To address this, a $CO_2$ polishing reactor that could decrease the $CO_2$ content can be added to the HGC unit of the gasifier side (see Fig. 14).

Since aluminosilicates were able to reduce the alkali concentrations to the sub $ppm_v$ range in the sorption experiments at 650 °C, the gas does not have to be cooled down before alkali cleaning. Since HCl is released during alkali binding into aluminosilicates (reaction (8), HCl cleaning must be carried out downstream in the process. A hot gas filter to remove particles is integrated after the alkali cleaning unit operating at 650 °C. It is important that the alkali cleaning is carried out before the filter so that it does not become clogged due to the condensation of alkali components. Afterwards, the gas reaches the $H_2S$ sorption reactor utilizing $Ce_2O_3$, BaO-, or SrO-based sorbents. To ensure the cracking of tar, which is not subject of the present investigations, the gas is lead through another reactor operating at 650 °C. Since a sufficient HCl reduction by BaO- or SrO-based sorbents could not be confirmed experimentally, adsorption by alkali carbonates is proposed. For successful HCl purification with $Na_2CO_3$, the temperature has to be lowered to 450 °C in a heat exchanger. At temperatures above 550 °C the sorption of HCl is not feasible as Na-based sorbents will release some of the chlorine as NaCl. The gas temperature can then be adjusted in another heat exchanger according to the conditions of the downstream equipment.

## 4. Summary and conclusions

Equilibrium calculations with FactSage were conducted for the hot gas cleaning unit of the GICO gasifier, proving that SrO- and BaO-based sorbents not only sufficiently reduced the $H_2S$, but also the HCl concentration into the sub $ppm_v$ range. Furthermore, aluminosilicates could reduce the concentration of alkali chlorides below 1 $ppm_v$.

In order to verify the modeling results, a test rig has been set up for sour gas sorption ($H_2S$ + HCl) using different metal oxides in a fixed bed. In this work, a simultaneous recording of the intensity and concentration curves of $CO_2$, $H_2S$ and $H_2$ was achieved using mass spectrometry. Furthermore, water was used in all sorption experiments, which counteracts the binding of $H_2S$ (reaction (1). With this setup, a reduction of the inorganic trace substance $H_2S$ below 1 $ppm_v$ could be detected for several hours ($Ce_2O_3$: 5 h, 90Ca10Ba: 2 h) at 650 °C which is considered sufficient to prevent catalyst poisoning. $Ce_2O_3$ and 90Ca10Ba can therefore be recommended for $H_2S$ sorption from a thermodynamic point of view. Moreover, due to the simultaneous reaction between $Ce_2O_3$, respectively BaO, and $CO_2$, a further shift to higher hydrogen concentrations could be observed by the water gas shift reaction. Zinc titanate, the most effective conventional sulfur sorbent tested, only

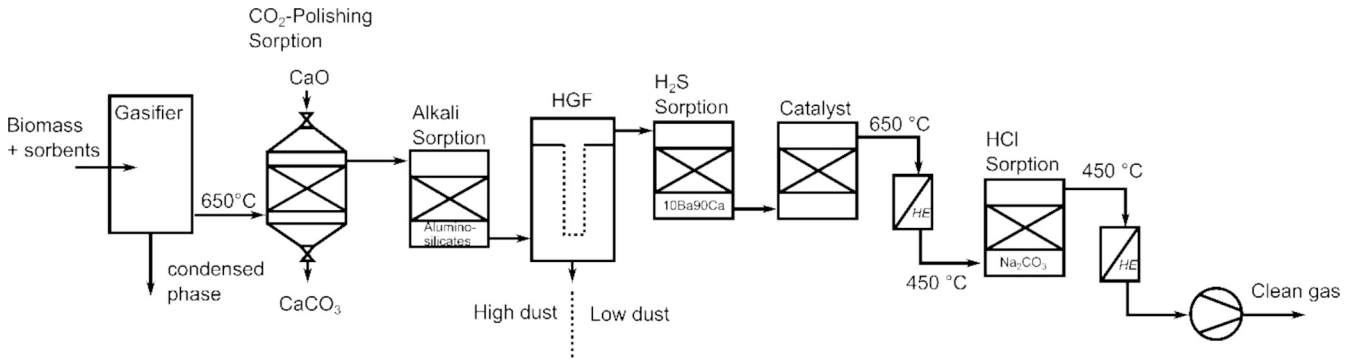


**Fig. 14.** Layout of a HGC for the GICO process.

reduced $H_2S$ levels to around 7 $ppm_v$.

On the other hand, 90Ca10Ba was not able to reduce the HCl concentration to a large extent. Concentrations could only be reduced from 50 to 40 $ppm_v$. Thus, contrary to initial thermodynamic calculations, this sorbent cannot be recommended for the sorption of $H_2S$ and HCl simultaneously. The reasons for this phenomenon require further investigation. It may be related to the reaction kinetics between HCl and the sorption material, or it could indicate a need for improvements to the database. Consequently, it is proposed to remove HCl in a separate cleaning step at lower temperatures, e.g., on alkali carbonates at 450 °C.

It was found that six aluminosilicates were effective in reducing KCl levels to below 1 $ppm_v$, with four of them achieving concentrations below 400 $ppb_v$ after 20 h at 650 °C. Since HCl is released when KCl is embedded using aluminosilicates, it is advisable to remove KCl before HCl.

## CRediT authorship contribution statement

**Markus Kopsch:** . **Patrick Schuster:** . **Elena Yazhenskikh:** Writing – review & editing. **Jürgen Sitzmann:** Writing – review & editing. **Michael Müller:** Writing – review & editing, Project administration.

## Declaration of competing interest

The authors declare the following financial interests/personal relationships which may be considered as potential competing interests: Markus Kopsch reports financial support was provided by European Union. Patrick Schuster reports a relationship with Research Centre Jülich that includes: employment. Elena Yazhenskikh reports a relationship with Research Centre Jülich that includes: employment. Michael Mueller reports a relationship with Research Centre Jülich that includes: employment. Juergen Sitzmann reports a relationship with Calida Cleantech GmbH that includes: board membership. If there are other authors, they declare that they have no known competing financial interests or personal relationships that could have appeared to influence the work reported in this paper.

## Acknowledgements

This work has received funding from the European Union's Horizon 2020 research and innovation program (Grant Agreement No.: 101006656). Further information are available at: https://www.gicoproject.eu/. We thank the colleagues of ZEA 3 of Forschungszentrum Jülich for chemical analysis.

## Data availability

Data will be made available on request.

## References

[1] Ngo T, Chiang KY, Liu CF, et al. Hydrogen production enhancement using hot gas cleaning system combined with prepared Ni-based catalyst in biomass gasification. Int J Hydrogen Energy 2021;46(20):11269–83. https://doi.org/10.1016/j.ijhydene.2020.08.279.

[2] Marcantonio V, Müller M, Bocci E. A Review of Hot Gas cleaning Techniques for Hydrogen Chloride Removal from Biomass-Derived Syngas. Energies 2021;14(20):6519. https://doi.org/10.3390/en14206519.

[3] Buchireddy PR, Peck D, Zappi M, et al. Catalytic Hot Gas Cleanup of Biomass Gasification producer Gas via Steam Reforming using Nickel-Supported Clay Minerals. Energies 2021;14(7):1875. https://doi.org/10.3390/en14071875.

[4] Stemmler M (2010) Chemische Heißgasreinigung bei Biomassevergasungsprozessen. Fakultät für Maschinenwesen. RWTH Aachen University, PhD-Thesis. Schriften des Forschungszentrums Jülich : Reihe Energie & Umwelt, Bd. 90, Aachen.

[5] Porbatzki D, Stemmler M, Müller M. Release of inorganic trace elements during gasification of wood, straw, and miscanthus. Biomass Bioenergy 2011;35:S79–86. https://doi.org/10.1016/j.biombioe.2011.04.001.

[6] Union E. Homepage GICO Project-GICO Process. Accessed 14.07.2024. https://www.gicoproject.eu/gico-process/. Accessed 14 Jul, 2024; 2021.

[7] Westmoreland PR, Harrison DP. Evaluation of candidate solids for high-temperature desulfurization of low-Btu gases. Environ Sci Technol 1976;10(7):659–61. https://doi.org/10.1021/es60118a010.

[8] Furimsky E, Yumura M. Solid adsorbents for removal of hydrogen sulphide from hot gas 1985. https://doi.org/10.4095/302594.

[9] Vamvuka D, Arvanitidis C, Zachariadis D. Flue Gas Desulfurization at High Temperatures: a Review. Environmental Engineering Science 2004;21(4):525–48. https://doi.org/10.1089/1092875041358557.

[10] Stemmler M, Tamburro A, Müller M. Laboratory investigations on chemical hot gas cleaning of inorganic trace elements for the "UNIQUE" process. Fuel 2013;108:31–6. https://doi.org/10.1016/j.fuel.2011.05.027.

[11] Focht GD, Ranade PV, Harrison DP. High-temperature desulfurization using zinc ferrite: Reduction and sulfidation kinetics. Chemical Engineering Science 1988;43(11):3005–13. https://doi.org/10.1016/0009-2509(88)80053-8.

[12] Diego LF, García-Labiano F, Adánez J, et al. Factors Affecting the H 2 S Reaction with Noncalcined Limestones and Half-Calcined Dolomites. Energy Fuels 1999;13(1):146–53. https://doi.org/10.1021/ef980145f.

[13] Katalambula H, Bawagan A, Takeda S. Mineral attachment to calcium-based sorbent particles during in situ desulfurization in coal gasification processes. Fuel Processing Technology 2001;73(2):75–93. https://doi.org/10.1016/S0378-3820(01)00200-4.

[14] Akiti T, Constant K, Doraiswamy L, et al. Development of an advanced calcium-based sorbent for desulfurizing hot coal gas. Advances in Environmental Research 2001;5(1):31–8. https://doi.org/10.1016/S1093-0191(00)00039-3.

[15] Katalambula H, Escallón MM, Takeda S. Influence of Ca-based Sorbent Particle size on the Occurrence of Solid−Solid Reactions during in-Situ Desulfurization of the Coal-Derived Gas. Energy Fuels 2001;15(2):317–23. https://doi.org/10.1021/ef000162g.

[16] Hartman M, Svoboda K, Trnka O, et al. Reaction between Hydrogen Sulfide and Limestone Calcines. Ind Eng Chem Res 2002;41(10):2392–8. https://doi.org/10.1021/ie010805v.

[17] Álvarez-Rodríguez R, Clemente-Jul C. Hot gas desulphurisation with dolomite sorbent in coal gasification. Fuel 2008;87(17–18):3513–21. https://doi.org/10.1016/j.fuel.2008.07.010.

[18] Sotirchos SV, Smith AR. Performance of Porous CaO obtained from the decomposition of calcium-enriched bio-oil as Sorbent for $SO_2$ and $H_2S$ Removal. Ind Eng Chem Res 2004;43(6):1340–8. https://doi.org/10.1021/ie034176w.

[19] Stemmler M, Tamburro A, Müller M. Thermodynamic modelling of fate and removal of alkali species and sour gases from biomass gasification for production of biofuels. Biomass Conv Bioref 2013;3(3):187–98. https://doi.org/10.1007/s13399-013-0073-7.

[20] Zeng Y, Kaytakoglu S, Harrison D. Reduced cerium oxide as an efficient and durable high temperature desulfurization sorbent. Chemical Engineering Science 2000;55(21):4893–900. https://doi.org/10.1016/S0009-2509(00)00117-2.

[21] Flytzani-Stephanopoulos M, Sakbodin M, Wang Z. Regenerative adsorption and removal of $H_2S$ from hot fuel gas streams by rare earth oxides. Science (New York, NY) 2006;312(5779):1508–10. https://doi.org/10.1126/science.1125684.

[22] Marcantonio V, Bocci E, Ouweltjes JP, et al. Evaluation of sorbents for high temperature removal of tars, hydrogen sulphide, hydrogen chloride and ammonia from biomass-derived syngas by using Aspen Plus. International Journal of Hydrogen Energy 2020;45(11):6651–62. https://doi.org/10.1016/j.ijhydene.2019.12.142.

[23] A. Hatunoglu, V. Marcantonio, E. Ciro et al. (2021) D.2.4. High temperature secondary sorbents selection for inorganic compounds removal and related lab scale fixed bed reactor performance. EU Blaze Project Report, L'Aquila.

[24] Han K, Li X, Qi J, et al. Synergistic effect of additives and blend on sulfur retention, on release and ash fusibility during combustion of biomass briquettes. International Journal of Green Energy 2021;18(2):187–202. https://doi.org/10.1080/15435075.2020.1847116.

[25] Gehrig M, Wöhler M, Pelz S, et al. Kaolin as additive in wood pellet combustion with several mixtures of spruce and short-rotation-coppice willow and its influence on emissions and ashes. Fuel 2019;235:610–6. https://doi.org/10.1016/j.fuel.2018.08.028.

[26] Punjak WA, Shadman F. Aluminosilicate sorbents for control of alkali vapors during coal combustion and gasification. Energy Fuels 1988;2(5):702–8. https://doi.org/10.1021/ef00011a017.

[27] Dou B, Shen W, Gao J, et al. Adsorption of alkali metal vapor from high-temperature coal-derived gas by solid sorbents. Fuel Processing Technology 2003;82(1):51–60. https://doi.org/10.1016/s0378-3820(03)00027-4.

[28] Uberoi M, Punjak WA, Shadman F. The kinetics and mechanism of alkali removal from flue gases by solid sorbents. Progress in Energy and Combustion Science 1990;16(4):205–11. https://doi.org/10.1016/0360-1285(90)90029-3.

[29] Zheng Y, Jensen PA, Jensen AD. A kinetic study of gaseous potassium capture by coal minerals in a high temperature fixed-bed reactor. Fuel 2008;87(15–16):3304–12. https://doi.org/10.1016/j.fuel.2008.05.003.

[30] de Riese T, Eckert D, Hakim L, et al. Modelling the Capture of Potassium by Solid Al-Si Particles at Pulverised fuel Conditions. Fuel 2022;328:125321. https://doi.org/10.1016/j.fuel.2022.125321.

[31] Fujita S, Suzuki K, Mori T, et al. A New Technique to Remove Hydrogen Chloride Gas at High Temperature using Hydrogrossular. Ind Eng Chem Res 2003;42(5):1023–7. https://doi.org/10.1021/ie020158n.

[32] Khaled KF, Abdel-Rehim SS, Sakr GB. On the corrosion inhibition of iron in hydrochloric acid solutions, Part I: Electrochemical DC and AC studies. Arabian Journal of Chemistry 2012;5(2):213–8. https://doi.org/10.1016/j.arabjc.2010.08.015.

[33] Verdone N, de Filippis P. Reaction kinetics of hydrogen chloride with sodium carbonate. Chemical Engineering Science 2006;61(22):7487–96. https://doi.org/10.1016/j.ces.2006.08.023.
[34] Li Y, Wu Y, Gao J. Study on a New Type of HCl-Removal Agent for High-Temperature cleaning of Coal Gas. Ind Eng Chem Res 2004;43(8):1807–11. https://doi.org/10.1021/ie034217o.
[35] Chyang C-S, Han Y-L, Zhong Z-C. Study of HCl Absorption by CaO at High Temperature. Energy & Fuels 2009;23(8):3948–53. https://doi.org/10.1021/ef900234p.
[36] Abbasian J, Wangerow JR, Hill AH. Effect of HCl on sulfidation of calcium oxide. Chemical Engineering Science 1993;48(15):2689–95. https://doi.org/10.1016/0009-2509(93)80181-O.
[37] Fujita S, Suzuki K, Shibasaki Y, et al. Synthesis of hydrogarnet from molten slag and its hydrogen chloride fixation performance at high temperature. J Mater Cycles Waste Manag 2002;4(1):70–6. https://doi.org/10.1007/s10163-001-0059-6.
[38] Fujita S, Suzuki K, Ohkawa M, et al. Reaction of Hydrogrossular with Hydrogen Chloride Gas at High Temperature. Chem Mater 2001;13(8):2523–7. https://doi.org/10.1021/cm000863r.
[39] Stemmler M, Müller M. D.4.1. Report on sorbents for alkali and sour gas removal. EU GreenSyngas-Project Report, Jülich 2010.
[40] Bale CW, Bélisle E, Chartrand P, et al. FactSage thermochemical software and databases, 2010–2016. Calphad 2016;54:35–53. https://doi.org/10.1016/j.calphad.2016.05.002.
[41] Yazhenskikh E, Jantzen T, Hack K, et al. A new multipurpose thermodynamic database for oxide systems 2019;Rasplavy(2):116–24. https://doi.org/10.1134/S0235010619010237.
[42] Kopsch M, Lebendig F, Yazhenskikh E, et al. Effect of HTC and Water-Leaching of Low-Grade Biomasses on the Release Behavior of Inorganic Constituents in a Calcium Looping Gasification Process at 650 °C. Energy Fuels 2024;38(17):16504–19. https://doi.org/10.1021/acs.energyfuels.4c02833.
[43] Wolf KJ, Müller M, Hilpert K, et al. Alkali Sorption in Second-Generation Pressurized Fluidized-Bed Combustion. Energy & Fuels 2004;18(6):1841–50. https://doi.org/10.1021/ef040009c.
[44] Escobar I, Müller M. Alkali Removal at about 1400 °C for the Pressurized Pulverized Coal Combustion combined Cycle. 2. Sorbents and Sorption Mechanisms. Energy & Fuels 2007;21(2):735–43. https://doi.org/10.1021/ef0605145.
[45] Weber CM (2008) Untersuchungen zum Alkaliverhalten unter Oxycoal-Bedingungen. Fakultät für Maschinenwesen. RWTH Aachen University, PhD-Thesis. Schriften des Forschungszentrums Jülich : […], Reihe Energie & Umwelt, Bd. 24, Aachen.
[46] Wolf KJ. Untersuchungen zur Freisetzung und Einbindung von Alkalimetallen bei der reduzierenden Druckwirbelschichtverbrennung. Fakultät für Maschinenwesen: RWTH Aachen University, PhD-Thesis, Aachen; 2003.
[47] van der Kemp W, Blok JG, van der Linde PR, et al. Binary alkaline earth oxide mixtures: Estimation of the excess thermodynamic properties and calculation of the phase diagrams. Calphad 1994;18(3):255–67. https://doi.org/10.1016/0364-5916(94)90032-9.
[48] Brauer G, editor. Handbuch der präparativen anorganischen Chemie. In drei Bänden, 3. umgearb. Aufl. Stuttgart: Enke; 1978.
[49] Mayernick AD, Li R, Dooley KM, et al. Energetics and Mechanism for $H_2S$ Adsorption by Ceria-Lanthanide mixed Oxides: Implications for the Desulfurization of Biomass Gasifier Effluents. J Phys Chem C 2011;115(49):24178–88. https://doi.org/10.1021/jp206827n.
[50] Mullins DR, McDonald TS. Adsorption and reaction of hydrogen sulfide on thin-film cerium oxide. Surface Science 2007;601(21):4931–8. https://doi.org/10.1016/j.susc.2007.08.007.